Crystal Structure of a Zinc-Activated Variant of Human Carbonic Anhydrase I, CA I Michigan 1: Evidence for a Second Zinc Binding Site Involving Arginine Coordination

Marta Ferraroni,[‡] Silvia Tilli,[‡] Fabrizio Briganti,*[,‡] W. Richard Chegwidden,*[,§] Claudiu T. Supuran,[‡] Karin E Wiebauer,[||] Richard E. Tashian,[||] and Andrea Scozzafava[‡]

Dipartimento di Chimica, Laboratorio di Chimica Bioinorganica, Università degli Studi di Firenze, Via della Lastruccia, 5, I-50019 Sesto Fiorentino, Italy, Lake Erie College of Osteopathic Medicine, 1858 West Grandview Boulevard, Erie, Pennsylvania 16509, and Department of Human Genetics, University of Michigan Medical School, Ann Arbor, Michigan 48109

Received November 12, 2001; Revised Manuscript Received February 27, 2002

ABSTRACT: The human genetic variant carbonic anhydrase I (CA I) Michigan 1 results from a single point mutation that changes His 67 to Arg in a critical region of the active site. This variant of the zinc metalloenzyme appears to be unique in that it possesses an esterase activity that is specifically enhanced by added free zinc ions. We have determined the three-dimensional structure of human CA I Michigan 1 by X-ray crystallography to a resolution of 2.6 Å. In the absence of added zinc ions, the mutated residue, Arg 67, points out of the active site, hydrogen bonding with the carboxylate of Asn 69. This contrasts with the orientation of His 67, in the native isozyme, which points into the active site. The orientations of His 94, His 96, and His 119, that coordinate the catalytic zinc ion, and of the catalytically critical Thr 199−Glu 106 hydrogen bonding system, are largely unchanged in the mutant. The structure of an enzyme adduct with a second zinc bound was determined to a resolution of 2.0 Å. The second zinc ion is coordinated to His 64, His 200, and Arg 67. This arginine residue reverses its orientation on zinc binding and turns into the active site. The residues at these three positions have been implicated in determining the specific kinetic properties of native CA I. This is, to our knowledge, the first example of a zinc ion coordinating with an arginine residue in a Zn(II) enzyme.

Carbonic anhydrase (CA[1]; EC 4.2.1.1) catalyzes the interconversion of carbon dioxide and bicarbonate ($CO_2 + H_2O \leftrightarrow HCO_3^- + H^+$). It occurs in three distinct gene families, α, *β*, and *γ*, which are variously expressed in virtually all living organisms. In vertebrates, only the α-genes are known to be present. These encode 14 isoforms, including 11 active isozymes, which are numbered in the sequence in which they were discovered. The active isozymes are all monomeric metalloproteins containing one catalytically essential zinc ion per polypeptide chain ($M_r \sim 29$ kDa). (For an overview of the α-CA isozymes, see ref *1*.)

Since the hydration of CO_2 is so fundamental in living organisms, the CA isozymes participate in numerous physiological processes (*1*). In the human red cell, CA I and CA II are expressed in high concentrations, especially CA I, which is the next most abundant protein to hemoglobin (∼13 mg/g of Hb). Here their roles lie in the transport and elimination of CO_2 and in acid−base balance (*1, 2*).

The X-ray structures of all of the α-CA isozymes resolved to date have shown that the single catalytic zinc ion is coordinated to three histidines and a water molecule/hydroxide ion (*3*−*7*). The catalytic mechanism of α-carbonic anhydrases has been investigated through kinetic, spectroscopic, and structural studies. The CO_2 hydration reaction is initiated by nucleophilic attack of the zinc-bound hydroxide ion on the CO_2 molecule, followed by the bidentate coordination to the metal ion of the bicarbonate product. This bicarbonate is subsequently released into solution on the binding of a new water molecule to the Zn(II) ion. The catalytically active, zinc-hydroxide form of the enzyme is restored through proton transfer to bulk solvent. (For reviews of the mechanism, see refs *8*−*10*.)

Human CA II, which is one of the fastest enzymes known, has a turnover number that is several orders of magnitude higher than the maximum rate of proton transfer to water (*10*). This high rate is achieved by the somewhat faster immediate transfer of protons to buffer. This occurs either directly to certain small buffer molecules, or indirectly, via a proton acceptor "shuttling" group on the enzyme, to other buffer molecules that may not be able to penetrate the active site cavity to sufficient depth, or with appropriate orientation, to provide an effective shuttle. His 64 acts as this shuttling

* Address correspondence to W.R.C. at Lake Erie College of Osteopathic Medicine, 1858 West Grandview Boulevard, Erie, PA 16509. Telephone: (814) 866-8167. FAX: (814) 866-8411. E-mail: wrchegwidden@lecom.edu or to F.B. at Dipartimento di Chimica, Università degli Studi di Firenze, Via della Lastruccia 5, I-50019 Sesto Fiorentino, Italia. Telephone: +39-055-4573248. FAX: +39-055-4573235. Email: fabrizio.briganti@unifi.it.

[‡] Università degli Studi di Firenze.

[§] Lake Erie College of Osteopathic Medicine.

[||] University of Michigan Medical School.

[1] Abbreviations: CA, carbonic anhydrase; HCA, human carbonic anhydrase; CA I M1, carbonic anhydrase I Michigan 1.

10.1021/bi0120446 CCC: $22.00
Published on Web 04/24/2002

group in CA II (*11*−*13*). Moreover, several molecules, such as histamine, have recently been found to further increase the activity of CA II. The X-ray structure of the CA II−histamine adduct shows that this molecule can actively participate in the proton shuttling process, thus augmenting the possible pathways of proton transfer and therefore the catalytic rate (*14*).

In CA I, which possesses about one-fifth of the activity of CA II, the situation is less clear. In this isozyme, the pK_a of His 64 is too low for efficient proton transfer (*15*), and the precise pathway or pathways of protons involving shuttle groups remain to be established (*10*).

Several site-directed mutations of active site residues of HCA II, resulting in changes of CO_2 hydration as well as esterase activity, have been extensively studied, permitting identification of amino acid side residues that play important roles in catalysis. Similar studies on HCA I have yielded intriguing results, although attempts to elucidate the basis for the catalytic differences between CA I and CA II have not yet proved entirely conclusive.

CA I and CA II can also act on other carbonyl systems, such as esters and aldehydes (*16*). There is a preponderance of evidence that catalysis of both ester hydrolysis and aldehyde hydration also occurs by a zinc-hydroxide mechanism similar to that outlined above for the CO_2 hydration reaction (*10*).

A number of naturally occurring variants of mammalian CA isozymes have been reported (*17*, *18*). One variant of human CA I (CA I Michigan 1) has attracted particular interest, since it provides an example of a point mutation that results in true metal ion activation of the gene product. This variant was discovered in three generations of a European Caucasian family residing in Michigan (*19*). Although its CO_2 hydration and esterase activities appeared to be within the normal range, when its esterase activity toward α- or β-naphthyl acetate was tested in the presence of the double zinc salt of 4′-amino-2′,5′-dimethoxybenzanilide (Blue RR) as an azo dye coupler, a large enhancement was observed. This suggested that the zinc ions dissociating from the dye complex were enhancing the esterase activity of the mutant isozyme. Further investigation showed that the esterase activity of the variant toward β-naphthyl acetate was enhanced 10-fold at a Zn(II) concentration of 10^{-4} M, and was not observed with other divalent metal ions, i.e., Co^{2+}, Cu^{2+}, Mg^{2+}, or Ni^{2+} (*20*, *21*). More recent studies revealed that, although CA I Michigan 1 was inhibited by heterocyclic sulfonamides in a manner similar to native CA I, its affinity for several aromatic sulfonamides was much lower (*22*).

The variant CA I Michigan 1 is the consequence of a single point mutation (CAT to CGT) resulting in the amino acid substitution His67Arg, located in the active site of the molecule (*23*). It provides a clear-cut example that a single amino acid substitution within the active site of a metalloenzyme, although not directly involved in the coordination of the catalytic metal, may critically affect both its catalytic and its inhibition properties. A histidine at position 67 has also been observed in a processed CA I gene isolated from a single human placenta (*24*).

We have crystallized the CA I Michigan 1 variant isozyme and now report the determination of its X-ray crystallographic structure, both in the presence and in the absence of a second bound zinc ion. The structures reported here may not only shed new light on the metal activation mechanism of CA I Michigan 1, but also provide new insight into the catalytic mechanism of CO_2 hydration by the α-CAs, and the molecular basis of the catalytic differences between the CA I and CA II isozymes.

MATERIALS AND METHODS

Buffers, 4-nitrophenylacetate, β-naphthyl acetate, acetonitrile, were from Sigma-Aldrich and used without further purification. All the other chemicals were of the best purity available.

All buffers used in the kinetic measurements were brought to an ionic strength $\mu = 0.1$, by addition of Na_2SO_4.

Enzyme Preparation. The cDNA encoding human CA I Michigan 1 was produced from a human placental cDNA library by site-directed mutagenesis employing the overlap extension method (*25*). This was cloned into plasmid pKK233-2, which was then transformed into *Escherichia coli* JM109 cells. These were grown in LB medium containing 50 μg/mL of ampicillin, and enzyme synthesis was induced by the addition of 0.5 mM isopropyl thio-β-D-galactoside and 0.5 mM $ZnSO_4$, followed by incubation at 30 °C for 8−12 h.

CA I Michigan 1 was purified by affinity chromatography, using *p*-aminomethylbenzene sulfonamide (PAMBS) (*26*). Enzyme concentrations were determined spectrophotometrically using $\epsilon_{280} = 49$ mM^{-1} cm^{-1} based on MW = 30 000. Electrophoresis on a 10% polyacrylamide gel stained with Coomassie blue was used to confirm purity, which was greater than 95%.

The catalytic activity of the purified enzyme was checked by measuring the initial rates of hydrolysis of 4-nitrophenyl acetate at 25 °C. The assay medium contained 0.4 mM substrate, 10% (v/v) acetonitrile, 50 mM Tris/H_2SO_4 and 50 mM Na_2SO_4 buffer, pH 8.0 (*15*). The formation of product was monitored at the isosbestic point for the corresponding nitrophenol and nitrophenolate ion (348 nm). The apparent second-order rate constants, k_{enz} (k_{cat}/K_M), were calculated using $\epsilon_{348} = 5.15$ mM^{-1} cm^{-1} for the reaction with 4-nitrophenyl acetate.

Protein Crystallization and Data Collection. Crystals of CA I Michigan 1 were obtained using the hanging drop vapor diffusion method. The enzyme (5 μL of a 15 mg/mL solution in 10 mM Tris·SO_4) was mixed with 5 μL of a precipitant solution containing 25% (w/v) PEG 4000, LiCl 0.4 M, Tris·HCl 100 mM, pH 9.0, 10% ethylene glycol. The presence of ethylene glycol in the reservoir cocktail was essential to avoid crystal damage due to the transfer in a cryoprotectant solution. After a few days at 22 °C, crystals of dimensions up to 1 mm were formed. These crystals were cooled at 100 K directly from the hanging drop, and data, extending to a maximum resolution of 2.6 Å, were collected using a Cu Kα radiation from a rotating anode X-ray generator coupled with a SMART 1K CCD detector from Bruker. Data collection consisted of two runs at different φ values of 0.3 ω scans using a detector distance of 7 cm and a detector swing angle (2θ) of 25°. A total of 740 frames were collected with a exposure time of 180 s. The diffraction data were processed using SAINT and resulted in 17 329 unique observations, an R_{symm} of 0.094 and an overall completeness of 97.9%. Details of the data collection and processing are reported in Table 1.

Table 1: Data Collection and Processing Statistics for CA I Michigan 1 and CA I Michigan 1−$Zn(II)_2$ Adduct Structures

	CA I Michigan 1	CA I Michigan 1−$Zn(II)_2$
space group	$P2_12_12_1$	
unit cell dimension (Å)	$a = 62.50$, $b = 72.13$, $c = 121.54$	$a = 62.68$, $b = 71.36$, $c = 120.91$
molecules/ asymmetric unit	2	
V_m (Å^3/Da)	2.25	
resolution range (Å)	20−2.6	15−2.0
raw measurements	58 715	82 254
unique reflections	17 329	35 578
completeness	97.9	94.9
Rsymm(%)	9.4	8.5
average I/σ (I)	7.8	8.0
redundancy	3.3	2.3

The crystal space group was unequivocally assigned to be orthorombic $P2_12_12_1$ with unit cell dimensions parameters $a = 62.50$, $b = 72.13$, $c = 121.54$.

Assuming a molecular mass of about 30 kDa and two molecules in the asymmetric unit the V_m value was calculated to be 2.25 Å^3/Da corresponding to a solvent content of 45%.

To obtain the structure of the HCA I Michigan 1, $Zn(II)_2$ adduct, crystals of the enzyme were soaked in a solution containing 25% (w/v) PEG 4000, LiCl 0.4 M, Tris·HCl 100 mM, pH 9.0, 10% ethylene glycol and $ZnSO_4$ 5 mM for 5 h.

Data for this enzyme adduct, extending to a maximum resolution of 2.0 Å, were collected at 100 K using experimental conditions and instrumentation as previously described. Data collection consisted of one run of 0.3 ω scans. A total of 600 frames were collected with an exposure time of 120 s. Further details of data collection are reported in Table 1.

Structure Solution and Refinement. The structure of the CA I Michigan 1 variant was solved by molecular replacement with the program AmoRe from the CCP4 program suite applied to the 10−4 Å data with a Patterson radius of 22 Å using, as a model, the atomic coordinates of human CA I (1czm) deposited in the Brookhaven Protein Data Bank (*27*−*29*). The rotation function gave only one solution, whereas a translational search gave two solutions as predicted from the V_m value. A translation as a noncrystallographic symmetry operation was confirmed by an experimental Patterson map that showed a peak at 16 σ corresponding to the translation vector between the two molecules in the asymmetric unit found with AmoRe. Rigid body refinement lowered the R-factor from 36.3 to 33.2. The solution showed reasonable contacts, and the inspection of the $2F_o-F_c$ Fourier map revealed a good agreement of the model with the electronic density. The refinement was carried out with the program Refmac from the CCP4 program suite (*28*). Approximately 860 reflections (5% of the data) were randomly excluded from the data set and used to follow the progress of the refinement with the R_{free}. The model was manually rebuilt on an O2 Silicon Graphics workstation using the program Quanta between rounds of refinement calculations (*30*). Anisotropy was introduced in the refinement of the temperature factors for the metal ions in the active sites of the two independently refined molecules in the asymmetric unit. Solvent molecules were introduced in the model using ARP only if the electron densities were above the 3σ level in the difference map, and if they were consistent with peaks in $2F_o-F_c$ maps and satisfied hydrogen bonding requirements (*31*). Zinc ions and all their protein and nonprotein ligands were not subjected to any constraint.

Table 2: Structure Refinement Statistics for CA I Michigan1 and CA I Michigan 1−$Zn(II)_2$ Adduct Structures

	CA I Michigan 1	CA I Michigan 1−$Zn(II)_2$
resolution limits	20−2.6	15−2.0
proteins atoms	3981	3995
water atoms	302	444
metal ions and others	10	21
R (%)	19.7	19.7
R_{free}(%)	30.5	27.7
Stereochemistry		
	weight	rms
bond length (Å)	0.020	0.013
angle distance (Å)	0.050	0.046
planar 1−4 distance (Å)	0.050	0.093
Average B-factor (Å^2)		
molecule A		
overall	28.5	20.6
protein	28.0	19.5
solvent	35.7	29.6
metal	20.8	21.5
others	21.0	39.4
molecule B		
overall	27.1	19.2
protein	26.4	18.2
solvent	36.8	28.2
metal	19.9	20.7
others	14.0	27.5

Electron density maps for the adduct of CA I Michigan 1 with exogenous zinc ions were calculated using phases from the refined coordinates of CA I Michigan 1. Refinement of the structure was performed using the programs Refmac and ARP, as previously described, coupled with sessions of model rebuilding using the program Quanta. The last restrained refinement cycle gave an R_{factor} of 19.7 and an R_{free} of 28.2. Anisotropy was introduced in the refinement for the metal ions, sulfur atoms, and chloride ions. The quality of the structures was checked with the program PROCHECK, and the final coordinates have been deposited with the Protein database under accession numbers 1J9W and 1JV0. The statistics for refinements are reported in Table 2 (*32*).

The final model of CA I Michigan 1 was constituted from two independently refined molecules (molecule A and molecule B). It contains a total of 3981 protein atoms and 302 water molecules, and each molecule also contains one Zn(II) metal ion in the active site, with an ethylene glycol molecule bound to it. The first four amino acids in both of the two molecules were not introduced in the model, since the $2F_o-F_c$ map showed a lack of electron density corresponding to them. Side chains for residues LysA39, LysA45, LysA80, LeuA189, AsnA237, AspB9, LysB10, GluB14, LysB34, LysB80, GluB102, and HisB103 were not modeled for the same reason. Average overall B factor was 28.5 Å^2 for molecule A and 27.1 Å^2 for molecule B. In the Ramachandran plot, 84.3% of nonglycine or proline residues lie in the most favored regions of the plot, while 15.6% lie

Table 3: Bond Distances and Angles of the Catalytic Zn Ion Coordination Polyhedron

	distance X−Zn (Å)			X−Zn−H94			X−Zn−H96			X−Zn−H119			X−Zn−O1		
	CA I M1			CA I M1			CA I M1			CA I M1			CA I M1		
	Mol A	Mol B	CA I	Mol A	Mol B	CA I	Mol A	Mol B	CA I	Mol A	Mol B	CA I	Mol A	Mol B	CA I
His 94 Nϵ2	1.87	1.94	1.93				100.5	101.0	107.9	117.1	116.5	115.4	105.1	99.9	
His 96 Nϵ2	2.21	2.00	1.94							98.4	106.7	97.9	105.0	125.9	
His 119 Nδ2	2.18	2.04	1.90										126.5	107.3	
O1 (EGL)	1.74	1.75													

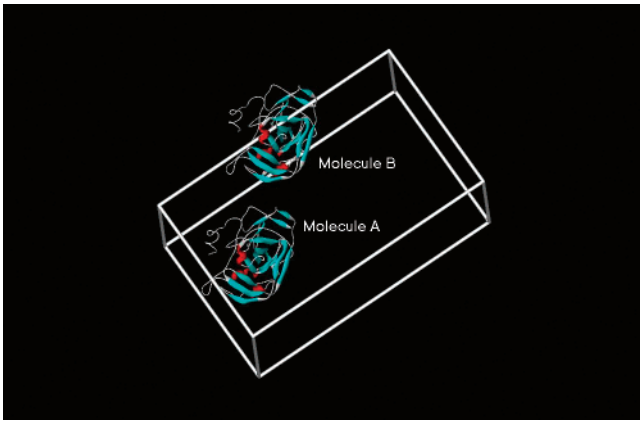

FIGURE 1: Asymmetric unit for the CA I Michigan 1 crystal structure.

within the allowed region (*32*). A total of 304 water molecules were introduced.

The final model of the Zn(II) adduct of CA I Michigan 1 contains a total of 3995 protein atoms and 442 water molecules in addition to three zinc ions, one chloride ion, and an ethylene glycol molecule for each protein molecule.

The first four amino acids and side chains for residues LysA39, LysA45, LysA80, LeuA189, AspB9, LysB10, GluB14, LysB34, LysB80, GluB102, and HisB103 were not introduced in the model. Alternative conformations were introduced for residues B15, B60, and B86.

RESULTS

As shown in Figure 1, two independent molecules, related by a translation operator, are present in the asymmetric unit of the new crystalline form obtained for CA I Michigan 1 (hereafter molecules A and B).

The overall three-dimensional structure of CA I Michigan 1 is very close to other published structures of HCA I (*3*, *33*), i.e. the global structure remains essentially unaltered by the single point mutation His67Arg, since the rms deviation between the structure of the native enzyme and that of the variant is 0.37 Å for molecule A and 0.34 Å for molecule B, respectively.

Figure 2 compares the relative positions of some of the active site residues of native HCA I (grey) and CA I Michigan 1 (green). An ethylene glycol molecule (present in the crystallization solution) in the CA I Michigan 1 displaces the metal-bound water molecule/hydroxide ion of the native enzyme.

The distances and the angles of the Zn(II) coordination polyhedron, compared to those of native HCA I, are reported in Table 3. No significant changes are observed.

The critical Thr 199−Glu 106 hydrogen bonding system, which appears to stabilize and orientate the catalytic zinc-bound hydroxide for catalysis (*34*), is present in both molecules A and B. In molecule A, the network through Tyr 7, His 64, and additional water molecules, observed by Kannan et al. (*3*), is evident, and extends to His 200, although not to Arg 67 that has substituted for His at that position in the native HCA I (Figure 3). The situation is somewhat different in molecule B, where the hydrogen bond network is interrupted between Tyr 7 and His 64, and a second hydrogen bond network involves Arg 67, His 200, Ser 65, and various water molecules (Figure 3).

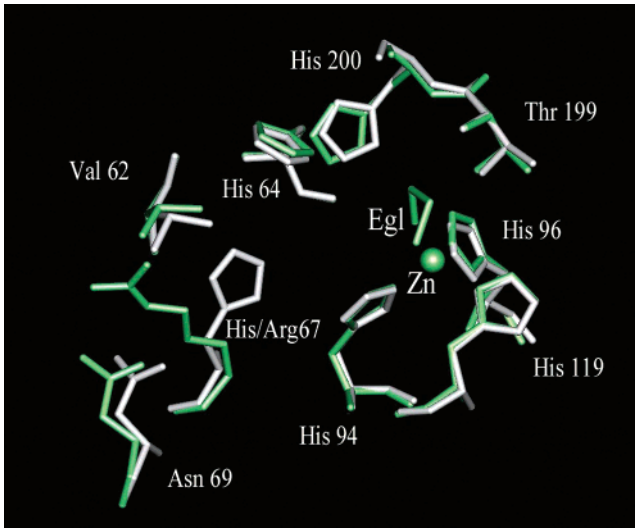

FIGURE 2: Least-squares superimposition of the most relevant active site residues of native human carbonic anhydrase I (His67) (grey structure) and CA I Michigan 1 (Arg67) (green structure).

The CA I Michigan 1 crystals were subsequently soaked in a solution containing $ZnSO_4$ to produce the crystal structure of the $Zn(II)_2$−enzyme adduct. The data collected with a resolution extending to 2.0 Å show relevant changes in the surroundings of the Arg 67, His 64, and His 200 residues. In particular, a new electron density corresponding to a second zinc ion coordinated to the side chains of His 200 and His 64 (also present in native HCA I) and to one of the guanidine nitrogen atoms of Arg 67 is now visible (Figure 4). An electron density corresponding to a chloride ion completes the coordination sphere of the second zinc ion.

Figure 5 shows the active site differences between CA I Michigan 1 with and without the second Zn(II) ion bound. The most significant change that occurs on the binding of the second Zn(II) ion to the active site of the variant is the rearrangement of Arg 67. In the $Zn(II)_2$−enzyme adduct, this residue has a different conformation from that found in the variant in the absence of the second zinc (Figure 5). We determined that between the two structures the rms for the Arg 67 side chain positions is 4.05 Å. In the CAI Michigan 1−$Zn(II)_2$ adduct the side chain of the mutated residue points

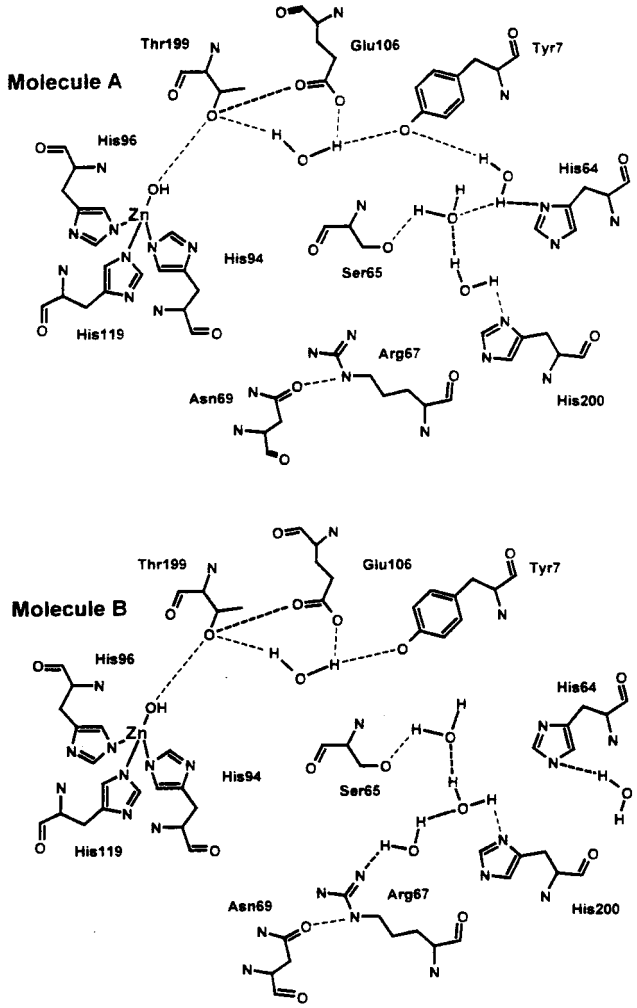

FIGURE 3: The active site hydrogen bond networks in molecules A and B of CA I Michigan 1.

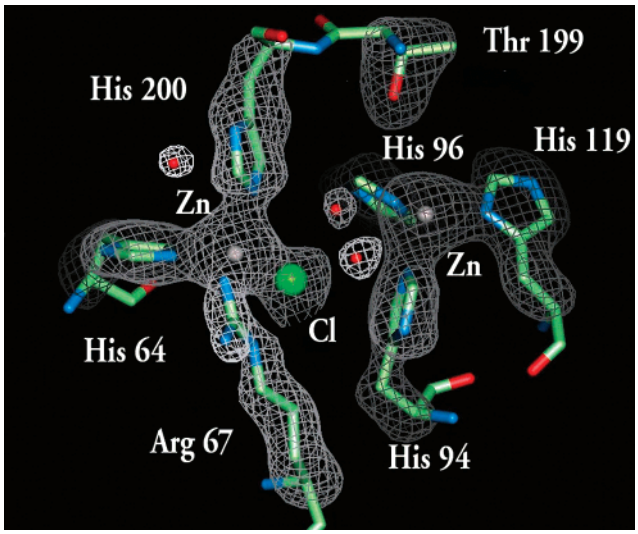

FIGURE 4: $2F_o-F_c$ electron density map contoured at 2σ, superimposed onto the final model of the CA I Michigan $1-Zn(II)_2$ adduct showing the active site region.

toward the interior part of the cavity, entering the coordination sphere of the second zinc ion, with bond lengths of 2.06 Å in molecule A and 2.12 Å in molecule B.

Within the active site, the catalytic zinc ion and its histidine ligands (His 94, His 96, and His 119) maintain the same

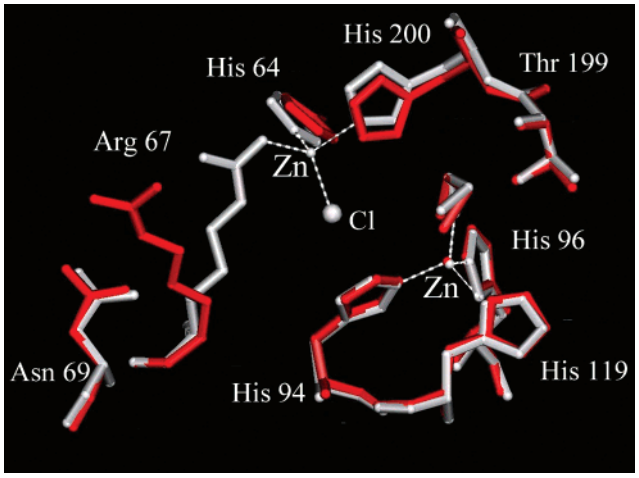

FIGURE 5: Least-squares superimposition of the most relevant active site residues of the CA I Michigan 1 variant before (red structure) and after (grey structure) soaking the crystals in a solution containing 5 mM Zn(II) ions.

conformation as in the native enzyme. Also in this structure, the coordination polyhedron of the catalytic zinc is completed by an ethylene glycol molecule that replaces the water/hydroxide moiety present in the wild-type enzyme. At the level of the ethylene glycol molecule the electron density shows some kind of disorder which was not modeled. The temperature factors for the ethylene glycol atoms are higher than those of the other zinc ligands, also indicating partial occupancy.

Another zinc ion was found on the enzyme surface, at about 50% occupancy. It is liganded to His 243, one chloride ion and two water molecules, with a tetrahedral distorted geometry. However, this third zinc ion is clearly bound very weakly, distally to the active site, and there is no evidence that it has any impact on active site configuration or catalytic activity.

In Table 4 the bond distances and angles of the second zinc coordination polyhedron present in the active site are reported.

In the CA I Michigan $1-Zn(II)_2$ adduct the active site hydrogen bond network is clearly different from that found in the structure of the variant without the second zinc. In contrast to the native enzyme, in both molecules A and B the hydrogen bond network is interrupted between Tyr 7 and His 64, the latter residue now being involved in the coordination of the second zinc ion. Some subtle differences between molecules A and B are present in the hydrogen bond network involving Arg 67, Gln 92, and Asn 69 as shown in Figure 6.

DISCUSSION

CA I Michigan 1 was the first mutant of a human CA isozyme to be reported, and is unique among CA variants in that one of its esterase activities is potently enhanced by addition of free zinc ions (*19*, *20*). In the absence of added zinc ions, Arg 67, in this variant, adopts a different conformation from its histidine counterpart in the native human CA I, pointing out of the active site. However, in the presence of added free zinc ions, when a second Zn(II) ion binds, this arginine turns into the active site to coordinate with it. Binding of this second zinc causes additional minor

Table 4: Bond Distances and Angles of Both Zn Ion Coordination Polyhedrons in the CA I Michigan 1−$Zn(II)_2$ Adduct

	X−Zn (Å)		X−Zn−H200		X−Zn−H64		X−Zn−R67		X−Zn−Cl	
distance	Mol A	Mol B	Mol A	Mol B	Mol A	Mol B	Mol A	Mol B	Mol A	Mol B
His 200 Nϵ2	2.11	2.26			109.2	98.8	110.7	111.1	101.3	102.6
His 64 Nϵ2	2.18	2.03					100.3	108.7	120.8	115.2
Arg 67	2.06	2.12							114.6	118.5
Cl^-	2.27	2.24								
					X−Zn−H96		X−Zn−H119		X−Zn−O1 (EGL)	
His 94 Nϵ2	2.04	1.98			102.7	101.9	110.8	115.6	117.7	123.1
His 96 Nϵ2	2.07	2.04					97.63	100.4	97.75	103.1
His 119 Nδ2	2.01	2.06							123.6	108.9
O1 (EGL)	1.82	1.72								

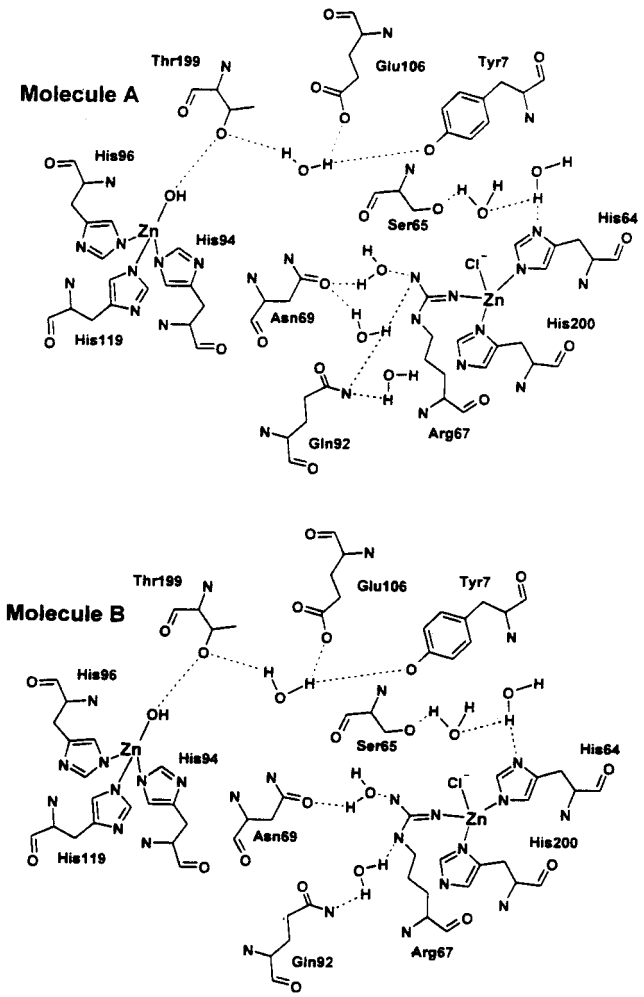

FIGURE 6: The hydrogen bond networks in molecules A and B of the CA I Michigan 1 variant obtained after soaking the crystals in a solution containing 5 mM Zn(II) ions.

conformational changes to several other active site residues, including His 64 and His 200, the other two residues to which it is coordinated. These active site modifications then result in an enhancement of the variant's esterase activity toward α- and β-naphthyl acetates. The residues in all three of these positions have been implicated in studies on the catalytic differences between native human CA I and the high activity CA II isozyme (*12*, *15*, *35*). Consequently, the study of this genetic variant is important not only in the elucidation of the mechanism of zinc ion esterase activation; it is also relevant to our understanding of the general active site geometry of the α-family of CA isozymes, of the mechanistic roles of these active site residues in CO_2 hydration, and of the molecular basis underlying the catalytic differences between the α-isozymes.

Preliminary studies on CA I Michigan 1 revealed no apparent change in the K_M value of the variant toward β-naphthyl acetate (*23*) when additional zinc was present, suggesting that the zinc-enhancement of the esterase activity may be attributed to a facilitation of the catalytic process rather than enhancement of substrate binding.

In native human CA I, His 200 is also involved in interaction with the ring structure of the classical clinical CA inhibitor acetazolamide (*36*). The substitution of Thr for His in this position resulted in weaker binding of dansylamide to this isozyme (*12*). This is consistent with the observation that the involvement of this residue in the coordination of the second zinc ion decreases the affinity of the variant for aromatic sulfonamides (*22*). Earlier data, monitoring the fluorescence patterns of dansyl sulphonamide (DNSA) in the presence and absence of added Zn(II) ions, suggested that the binding of the second zinc ion caused the DNSA to move to a more hydrophobic region of the active site (*20*). It is noteworthy in this context that, in crystals of the variant, an ethylene glycol molecule replaces the metal-bound water molecule/hydroxide ion of the native enzyme. Coordination of an alcohol molecule to the Zn(II) ion has not been reported for any other CA isozyme.

In native CA I, His 200 and His 67, along with Val 62, are all isozyme-specific residues that appear to contribute to this isozyme's unique kinetic features. Although the kinetic data suggest that some proton shuttling occurs in the native CA I, the route of shuttling is unclear. Indeed, non-Michaelis−Menten kinetic patterns for native human CA I have been interpreted as resulting from multiple pathways for a rate-limiting proton transfer from the active center to the bulk solvent (*38*). Notwithstanding, at high buffer concentrations, when rates of proton transfer are optimal, the CO_2−HCO_3^- interconversion step is probably rate-limiting in CA I (*35*).

His 200 is close to the zinc ion, and has been suggested as a candidate for a shuttling residue (*37*), but this is a matter for debate since its p*K* value, like that of His 64, is probably too low (*15*). Nonetheless, the CA I mutant His200Thr exhibits a decreased buffer specificity ratio (*12*), indicating a loss of shuttling capacity when the histidine is replaced. At the same time, other kinetic data suggest that His 200 stabilizes the enzyme−bicarbonate complex, thus decreasing the rate of bicarbonate dissociation from the enzyme (*12*). In contrast, His 67 and Val 62 appear to attenuate the rate of proton transfer (*12*), although their effect must be indirect

in view of their distance from the catalytic center. Thus, it appears that, in native human CA I, His 200, His 67, and Val 62 all behave in such a way as to prevent the enzyme from attaining its full catalytic potential (as does Phe 198 in CA III). Clearly, further investigation of the roles of these residues will be necessary before a complete picture of the catalytic process in CA I may be formulated.

Since both His 200 and Arg 67 are coordinated to the second zinc ion in CA I Michigan 1, it would seem axiomatic that a detailed kinetic analysis of this variant is likely to provide information pertinent to the formulation of this picture. While preliminary data suggest that the CO_2 hydration activity of the variant may be within the normal range, the assay techniques employed did not permit individual analysis of the separate components of the reaction pathway.

To our knowledge, this is the first report of a Zn(II) protein coordination sphere containing an arginine residue. Arginine residues are known to be present in the active sites of various Zn enzymes, such as carboxypeptidase A, leucine aminopeptidase, and alkaline phosphatase, where they play roles in substrate orientation and activation as well as transition state stabilization (*39*). Typically, the guanidino group of free arginine would ionize with a pK_a of around 12.5, although it is well-known that the local environment of a chemical group on a large molecule such as a protein may significantly affect its pK_a value, largely through dielectric and electrostatic effects (*40*). Similarly, metal ions can bind ligands at a pH well below their pK_a values largely due to inductive effects (*39*). However, since our structural determinations were undertaken at pH 9.0, coordination of Arg 67 to the second Zn(II) ion would require a notably large reduction, well in excess of three units, in the pK_a value of the arginine side chain.

Models for arginine-metal binding indicate a high affinity of guanidine ligands for metal ions such as Pt, Os, Co, and Cu (*41*, *42*). It has been suggested that the metal-induced enhancement of the coordinating ability of guanidines may be particularly relevant in hydrophobic biological environments, where electrophilic metal ions may compete better with the proton (*41*). For example, it was proposed that the guanidine group of Arg 74 in the Ni−Fe hydrogenase from *Desulfovibrio gigas* was an essential ligand for the Ni(III) complex (*43*); however, the X-ray structure of this enzyme subsequently showed this to be incorrect (*44*). Consequently, we believe that the structure presented here, of CA I Michigan 1 with the second zinc ion bound, is the first demonstrated example of arginine coordination to a metal ion in proteins.

In liver arginase, histidine has been reported to function as a base in facilitating the deprotonation of arginine, thus allowing entry of the neutral guanidium group into the metal ion coordination sphere (*45*). In the present structure, the nucleophilicity of Arg 67 is most probably enhanced by the presence of neighbors such as His 64 and His 200, which also bind to the same metal center.

Further kinetic and structural investigations are currently under way with a view to elucidating the mechanism of zinc ion activation of CA I Michigan 1, as well as furthering our understanding of the mechanism of native CA I and the roles played by particular active site residues in determining its isozyme-specific kinetic properties.

ACKNOWLEDGMENT

We wish to thank the Target Project on Biotechnologies CNR Italy.

REFERENCES

1. Chegwidden, W. R., and Carter, N. (2000) in *The Carbonic Anhydrases: New Horizons* (Chegwidden, W. R., Carter, N. D., and Edwards, Y. H., Eds.) pp 13−28, Birkhauser Verlag AG, Basel, Switzerland.
2. Swenson, E. R. (2000) in *The Carbonic Anhydrases: New Horizons.* (Chegwidden, W. R., Carter, N. D., and Edwards, Y. H., Eds.) pp 281−341, Birkhauser Verlag AG, Basel, Switzerland.
3. Kannan, K. K., Ramanadham, M., and Jones, T. A. (1984) *Ann. N. Y. Acad. Sci. 429*, 49−60.
4. Eriksson, A. E., Jones, T. A., and Liljas, A., (1988) *Proteins Struct. Funct. Genet. 4*, 274−282.
5. Eriksson, A. E., and Liljas, A., (1993) *Proteins Struct. Funct. Genet. 16*, 29−42.
6. Stams, T., Nair, S. K., Okuyama, T., Waheed, A., Sly, W. S., and Christianson, D. W. (1996) *Proc. Natl. Acad. Sci. U.S.A. 93*, 13589−13594.
7. Boriack-Sjodin, P. A., Heck, R. W., Liaipis, P. J., Silverman, D. N., and Christianson, D. W. (1995) *Proc. Natl. Acad. Sci. U.S.A. 92*, 10949−10953.
8. Silverman, D. N., and Lindskog, S. (1988) *Acc. Chem. Res. 21*, 30−36.
9. Lindskog, S. (1997) *Pharmacol. Ther. 74*, 1−20.
10. Lindskog, S., and Silverman, D. N. (2000) in *The Carbonic Anhydrases: New Horizons* (Chegwidden, W. R., Carter, N. D., and Edwards, Y. H. Eds.) pp 175−195, Birkhauser Verlag AG, Basel, Switzerland.
11. Tu, CK, Silverman, D. N., Forsman, C., Jonsson, B.-H.; Lindskog, S. (1989) *Biochemistry 28*, 7913−7918.
12. Engstrand, C., Jonsson, B.-H., and Lindskog, S. (1995) *Eur. J. Biochem. 229*, 696−702.
13. Duda, C., Tu, C., Qian, M., Laipis, P., Agbandje-McKenna, M., Silverman, D. N., and McKenna, R. (2001) *Biochemistry 40*, 1741−1748.
14. Briganti, F., Mangani, S., Orioli, P., Scozzafava, A., Vernaglione, G., and Supuran, C. T. (1997) *Biochemistry 36*, 10384−10392.
15. Campbell, I. D., Lindskog, S., and White, A. I. (1974) *J. Mol. Biol. 90*, 469−489.
16. Pocker, Y., and Sarkanen, S. (1978) *Adv. Enzymol. 47*, 149−274.
17. Tashian, R. E. (1992) *Adv. Genet. 30*, 321−357.
18. Venta, P. B. (2000) in *The Carbonic Anhydrases: New Horizons.* (Chegwidden, W. R., Carter, N. D., and Edwards, Y. H., Eds.) pp 403−412, Birkhauser Verlag AG, Basel, Switzerland.
19. Shaw, C. R., Syner, F. N., and Tashian, R. E. (1962) *Science 138*, 31−32.
20. Tashian, R. E., and Carter N. D. (1976) *Adv. Hum. Genet. 7*, 1−56.
21. Tashian, R. E., Kendall, A. G., and Carter, N. D. (1980) *Hemoglobin 4*, 6350651.
22. Briganti, F.; Chegwidden, W. R.; Scozzafava, A.; Supuran, C. T.; Tashian, R. E.; and Wiebauer, K. E. (1998) *Gene Fam. Isozyme. Bull. 31*, 43.
23. Chegwidden, W. R., Wagner, L. E., Venta, P. J., Bergenhem, N. C. H., Yu, Y. S. L., and Tashian, R. E. (1994) *Hum. Mutat. 4*, 294−296.
24. Chegwidden, W. R., Tashian, R. E., and Wiebauer, K. E. (2001) *Gene Fam. Isozyme. Bull. 34*, 31−35.
25. Chegwidden, W. R., Wiebauer, K. E., Venta, P. J., Bergenhem, N. C. H., and Tashian, R. E. (1995) *Isozyme Bull. 28*, 37.
26. Khalifah, R. G., Strader, D. J., Bryant, S. H., and Gibson, S. M. (1977) *Biochemistry 16*, 2241−2247.
27. Navaza, J. (1994) *Acta Crystallog. Sect. A 50*, 157−163.
28. Collaborative Computational Project, N. 4 (1994) *Acta Crystallogr. D50*, 760−763 (Abstract).

29. Berman, H. M., Westbrook, J., Feng, Z., Gilliland, G., Bhat, T. N., Weissig, H., Shindyalov, I. N., and Bourne, P. E. (2000) *Nucleic Acids Res. 28*, 235−242.
30. Quanta Simulation, Search, and Analysis, July 1997, San Diego: Molecular Simulations Inc.
31. Lamzin, V. S., and Wilson, K. S. (1993) *Acta Crystallogr. D49*, 129−147.
32. Laskowski, R. A., MacArthur, M. W., Moss, D. S., and Thornton, J. M(1993) *J. Appl. Crystallogr. 26*, 283−291.
33. Kannan, K. K., Notstrand, B., Fridborg, K., Lovgren, S., Ohlsson, A., and Petef, M. (1975) *Proc. Natl. Acad. Sci. U.S.A. 72*, 51−55.
34. Merz, K. M. (1990) *J. Mol. Biol. 214*, 799−802.
35. Behravan, G., Jonsson, B. H., and Lindskog, S. (1990) *Eur. J. Biochem. 190*, 351−357.
36. Chakravarty, S., and Kannan, K. K. (1994) *J. Mol. Biol. 243*, 298−309.
37. Stams, T., and Christianson, D. W. (2000) in *The Carbonic Anhydrases: New Horizons* (Chegwidden, W. R., Carter, N. D., and Edwards, Y. H. Eds.) pp 159−174, Birkhauser Verlag AG, Basel, Switzerland.
38. Ren, X., and Lindskog, S. (1992) *Biochim. Biophys. Acta 1120*, 81−86.
39. Holm, R. H., Kennepohl, P., and Solomon, E. I. (1996) *Chem. Rev. 96*, 2239−2314.
40. Cantor, C. R., and Schimmel, P. R. (1980) in *Biophysical Chemistry. Part I, The Conformation of Biological Macromolecules*, pp 42−51, W. H. Freeman and Co., New York.
41. Fairlie, D. P., Jackson, W. G., Skelton, B. W., Wen, H., White, A. H., Wickramasinghe, W. A., Woon, T. C., and Taube, H. (1997) *Inorg. Chem. 36*, 1020−1028.
42. Chicira, M., Inoe, M., Nagane, R., Harada, W., and Shindo, H. (1997) *J. Inorg. Biochem. 66*, 131−139.
43. Przybyla, A. E., Robins, J., Menon, N., and Peck, H. D. (1992) *FEMS Microbiol. Rev. 88*, 109−135.
44. Volbeda, A., Charon, M. H., Piras, C., Hatchikian, E. C., Frey, M., and Fontecilla-Camps, J. C. (1995) *Nature 373*, 580−587.
45. Khangulov, S. V., Sossong, T. M., Jr., Ash, D. E., and Dismukes, G. C. (1998) *Biochemistry 37*, 8539−8550.

BI0120446